

Despite Increased CD4⁺Foxp3⁺ Cells within the Infection Site, BALB/c IL-4 Receptor-Deficient Mice Reveal CD4⁺Foxp3-Negative T Cells as a Source of IL-10 in *Leishmania major* Susceptibility¹

Hisashi Nagase,^{2*} Kathryn M. Jones,* Charles F. Anderson,[†] and Nancy Noben-Trauth^{3*}

BALB/c IL-4R α ^{-/-} mice, despite the absence of IL-4/IL-13 signaling and potent Th2 responses, remain highly susceptible to *Leishmania major* substrain LV39 due exclusively to residual levels of IL-10. To address the contribution of CD4⁺CD25⁺ T regulatory (Treg) cells to IL-10-mediated susceptibility, we depleted CD4⁺CD25⁺ cells in vivo and reconstituted IL-4R α × RAG2 recipients with purified CD4⁺CD25⁻ T cells. Although anti-CD25 mAb treatment significantly decreased parasite numbers in IL-4R α ^{-/-} mice, treatment with anti-IL-10R mAb virtually eliminated *L. major* parasites in both footpad and dermal infection sites. In addition, IL-4R α × RAG2 mice reconstituted with CD4⁺ cells depleted of CD25⁺ Treg cells remained highly susceptible to infection. Analysis of *L. major*-infected BALB/c and IL-4R α ^{-/-} inflammatory sites revealed that the majority of IL-10 was secreted by the CD4⁺Foxp3⁻ population, with a fraction of IL-10 coming from CD4⁺Foxp3⁺ Treg cells. All T cell IFN- γ production was also derived from the CD4⁺Foxp3⁻ population. Nevertheless, the IL-4R α ^{-/-}-infected ear dermis, but not draining lymph nodes, consistently displayed 1.5- to 2-fold greater percentages of CD4⁺CD25⁺ and CD4⁺Foxp3⁺ Treg cells compared with the BALB/c-infected dermis. Thus, CD4⁺Foxp3⁻ T cells are a major source of IL-10 that disrupts IFN- γ activity in *L. major*-susceptible BALB/c mice. However, the increase in CD4⁺Foxp3⁺ T cells within the IL-4R α ^{-/-} dermis implies a possible IL-10-independent role for Treg cells within the infection site, and may indicate a novel immune escape mechanism used by *L. major* parasites in the absence of IL-4/IL-13 signaling. *The Journal of Immunology*, 2007, 179: 2435–2444.

L *eishmania major* infection in mice has proven to be a powerful model to dissect the immune processes that govern polarized Th1/Th2 cytokine responses. In susceptible BALB/c mice, an early burst of IL-4 after *L. major* infection drives Th2 polarization, impairs Th1 responses required for parasite elimination, and finally leads to fatal disease (1). In addition to IL-4, the related cytokine IL-13 has been also demonstrated as a factor for *L. major* susceptibility (2, 3). Based on this evidence, IL-4/IL-13 signaling through the shared IL-4R α -chain (IL-4R α) is considered to play a pivotal role in *L. major* susceptibility.

Inconsistent with the Th1/Th2 paradigm, BALB/c IL-4^{-/-} and IL-4R α ^{-/-} mice failed to control parasite growth of certain *L. major* substrains such as LV39 (2, 4) and NIH/Seidman (5), whereas IL-4R α ^{-/-} mice controlled other *L. major* substrains, including IR173 and V1 (2). These data imply the existence of ad-

ditional or alternative pathways for *L. major* disease progression in BALB/c mice.

Results from a number of groups now support the concept that IL-10 is an important susceptibility factor for *L. major*. In a previous report, we have shown that both IL-10 and IL-4R α signaling contribute to *L. major* susceptibility regardless of *L. major* substrains (6). In addition, Kane and Mosser (7) demonstrated fewer *L. major* parasites in IL-10^{-/-} mice on a susceptible BALB/c background. Moreover, in resistant C57BL/6 mice, IL-10 has been shown to be involved in maintaining a persistent *L. major* infection that may be required for maintaining immunological memory (8).

CD4⁺CD25⁺ T regulatory (Treg)⁴ cells control several autoimmune diseases via cell-cell interactions and soluble factors such as IL-10 and TGF- β (9, 10). Within the CD4⁺CD25⁺ Treg population, further classifications differentiate naturally occurring, thymic-derived Treg cells that express the transcription factor Foxp3 (11), and those that have been induced in the periphery via APC interactions, the cytokine milieu, or that are induced by the natural Treg population (12–16).

Several groups have explored the role of Treg cells in *L. major* infection. In resistant mice, IL-10 secretion from Treg cells was necessary for *L. major* substrain V1 parasite persistence following clinical cure in C57BL/6 mice (17). CD4⁺CD45RB^{low} T cells, which are enriched for CD4⁺CD25⁺ Treg cells, have been shown to cause susceptibility after transfer into SCID mice (18). In addition, Treg cells were shown to suppress both Th1 and Th2 differentiation early in *L. major* infection (19), but ultimately caused disease later in infection via secretion of several factors, including

*Department of Microbiology, Immunology and Tropical Medicine, George Washington University Medical Center, Washington, DC 20037; and [†]Laboratory of Parasitic Diseases, National Institute of Allergy and Infectious Diseases, National Institutes of Health, Bethesda, MD 20892

Received for publication June 23, 2006. Accepted for publication June 8, 2007.

The costs of publication of this article were defrayed in part by the payment of page charges. This article must therefore be hereby marked *advertisement* in accordance with 18 U.S.C. Section 1734 solely to indicate this fact.

¹ This work was supported by National Institutes of Health Grant AI054717 (to N.N.-T.).

² Current address: Infectionology and Immunology on Organ Transplants, Shinshu University Graduate School of Medicine, 3-1-1 Asahi, Matsumoto, 390-8621, Japan. E-mail address: hnagase@sch.md.shinshu-u.ac.jp

³ Address correspondence and request reprints to Dr. Nancy Noben-Trauth, Department of Microbiology, Immunology and Tropical Medicine, George Washington University Medical Center, Ross Hall, Room 407, 2300 Eye Street NW, Washington, DC 20037. E-mail address: nnoben@gwu.edu

⁴ Abbreviations used in this paper: Treg, T regulatory; C_T, cycle threshold; KO, knockout; LN, lymph node; pm, promastigote; qPCR, quantitative PCR; SLA, soluble *Leishmania* Ag.

IL-10 (20). Contrary to these findings, Aseffa et al. (21) reported that Treg cells protect against *L. major* infection, and that disease severity in susceptible BALB/c mice was exacerbated after depleting CD4⁺CD25⁺ Treg cells in vivo. In recent studies using bicistronic Foxp3 reporter mice, Anderson et al. (22) have shown that the nonhealing phenotype in C57BL/6 mice infected with *L. major* Seidman is due to IL-10 secretion from CD4⁺CD25⁻Foxp3⁻ T cells. Thus, the role of CD4⁺CD25⁺ Treg cells in susceptibility to *L. major* infection, particularly in BALB/c mice, remains unresolved.

In the study presented in this work, we evaluated the role of Treg cells in *L. major* in susceptible IL-4R α -deficient mice, which, in the absence of IL-4/IL-13 signaling, remain highly susceptible to *L. major* substrain LV39 due to IL-10. We used both the conventional footpad infection as well as the ear dermal infection model (23), which allows analysis of events occurring within the site of infection. Because IL-10 is the exclusive cytokine mediating susceptibility in IL-4R α ^{-/-} mice, we have the opportunity to dissect the conditions and the cells that invoke IL-10 responses to *L. major* infection in vivo.

Materials and Methods

Mice

Genetically pure BALB/c IL-4R α ^{-/-} mice were generated, as previously described (24). BALB/c IL-10^{-/-} mice (backcross $n = 8$) were provided by D. Rennick (DNAX Research Institute, Palo Alto, CA) and bred in our facility. IL-4R α \times IL-10 and IL-4R α \times RAG2 double-deficient mice were generated by crossing the parental strains and maintained under contract at Taconic Farms. All mice were maintained under specific pathogen-free conditions in the George Washington University Medical Center under protocols approved by the Institutional Animal Care and Use Committee.

Culture medium

Complete RPMI 1640 consisted of RPMI 1640 medium (Mediatech) supplemented with 10% FBS (Invitrogen Life Technologies), 1 mM sodium pyruvate, 2 mM L-glutamine, 0.05 μ M 2-ME, 100 U/ml penicillin, and 100 μ g/ml streptomycin.

Parasites

L. major substrain LV39 (MRHO/SU/59/P) promastigotes (pm) were cultured at 26°C in medium 199 supplemented with 20% heat-inactivated FCS (Gemini Bio-Products), 100 U/ml penicillin, 100 μ g/ml streptomycin, 2 mM L-glutamine, 40 mM HEPES, 0.1 mM adenine, and 5 μ g/ml hemin (M199/S). Infective stage metacyclic pm were isolated from stationary culture (5–7 days old) by Ficoll (FisherBiotec) density gradient method, as described previously (25). Mice were infected s.c. with 10⁵ purified metacyclics in the left hind footpad or with 2 \times 10⁴ metacyclics intradermally in the ear dermis, as previously described (23).

Parasite quantitation

Infected footpad tissue homogenates were prepared by using Teflon-coated microtissue grinder in 1.5-ml microfuge tubes containing 200 μ l of M199/S. Homogenates were serially diluted in a 96-well flat-bottom microtiter plate containing 50 μ l of rabbit blood agar (1.4% agar of Novy-MacNeal-Nicolle medium containing 30% defibrinated rabbit blood). One well was used for each 2-fold serial dilution. The number of viable parasites in each sample was determined from the highest dilution at which pm could be detected after 10 days of incubation at 26°C. Parasite numbers in the ear dermis were determined, as previously described (17). Briefly, the ventral and dorsal sheets of the infected ears were separated; deposited dermal-side down in DMEM containing 100 U/ml penicillin, 100 μ g/ml streptomycin, and 50 μ g/ml Liberase CI enzyme blend (Roche Diagnostic Systems); incubated for 2 h at 37°C; and homogenized using a Medi-Machine (DakoCytomation). The resultant ear homogenates were filtered using a 70- μ m pore-size cell strainer (Falcon Products) to exclude debris. Right and left ears were pooled for each individual mouse, and parasite numbers were calculated by dividing the total pm by two. The numbers of parasites in the local draining lymph nodes (LN; popliteal or retroaxillary) were also determined. The LN were removed, mechanically dissociated, and serially diluted in the rabbit blood agar plates, as described above.

In vitro stimulation and ELISAs

To measure *Leishmania*-specific cytokine responses, 6 \times 10⁵ draining LN cells were cultured in 96-well plates with 200 μ l of complete RPMI 1640 containing 25 μ g/ml soluble *Leishmania* Ags (SLA) prepared from LV39 metacyclic pm. Supernatants were harvested at 72 h after stimulation and assayed for cytokines. IFN- γ (Pierce) and IL-10 (R&D Systems) ELISAs were performed, according to manufacturers' instructions.

Antibodies

Anti-CD4-PerCP, -FITC; CyChrome (RM4-5); anti-CD25-PE, -allophycocyanin (3C7 and PC61); anti-IL-10-PE, -allophycocyanin (JES5-16E3); anti-IFN- γ -FITC, -allophycocyanin (XMG1.2); anti-IL-4-PE (11B11); and anti-CD103 (M290) were all purchased from BD Biosciences. The 3C7 and PC61 mAb recognize distinct epitopes on the CD25 molecule. Anti-Foxp3 (FJK-16s) labeled with FITC and PE was purchased from eBioscience. The anti-CD25 hybridoma (PC61.5.3, rat IgG1) was purchased from American Type Culture Collection. Anti-IL-10R (1B1.3a, rat IgG1) and control mAb (GL113, rat IgG1) hybridomas were provided by K. Moore (DNAX, Palo Alto, CA). The anti-CD25, anti-IL-10R, and control mAbs used in vivo were generated from ascites produced in nude mice and purified by ammonium sulfate precipitation and ion exchange chromatography (Harlan Bioproducts).

T cell transfers

For the adoptive transfer of CD4⁺CD25⁻ T cells, CD4⁺ T cells were enriched from naive IL-4R α ^{-/-} or IL-4R \times IL-10 spleen cells using SpinSep CD4 kit (StemCell Technologies) and the CD4⁺CD25⁻ cells purified by MACS (Miltenyi Biotec). IL-4R α \times RAG2 mice were reconstituted with 1 \times 10⁷ total CD4⁺ or CD4⁺CD25⁻ T cells by i.v. injection. One day after reconstitution, mice were intradermally infected with *L. major* LV39.

T cell stimulation and intracellular staining

Ear dermal homogenates were cultured overnight at 37°C in 600 μ l of complete RPMI 1640 in 48-well plates. The next day, the cells were stimulated with 10 ng/ml PMA and 500 ng/ml ionomycin in the presence of 3 mM monensin (BD Biosciences) for 4 h. Cells were washed; blocked with 5% normal mouse serum and 2.4G2 (10 μ g/ml), stained with cell surface markers, including anti-CD4 CyChrome, anti-CD25 allophycocyanin, and/or anti-CD103 FITC; and then cells were washed and fixed in 1 \times Fix/Perm solution for Foxp3 intranuclear staining for 1 h on ice or Cytofix/CytoPerm for 15 min for all other intracellular staining. The cells were washed and resuspended in permeabilization buffer (BD Biosciences or eBioscience), and then stained with combinations of anti-IFN- γ FITC, anti-IL-10 PE, or anti-Foxp3 FITC, and analyzed by FACS. For each sample, 300,000 total events were analyzed. The data were collected and analyzed using CellQuest software and a FACSCalibur flow cytometer or FACSDiva software and a FACSAria flow cytometer (BD Biosciences).

Quantitative RT-PCR

Total RNA was extracted from FACS-sorted CD4⁺ populations from BALB/c and IL-4R α ear dermis homogenates using the RNeasy micro kit (Qiagen). The sorted populations were CD4⁺CD25⁺CD103⁺, CD4⁺CD25⁻CD103⁺, and CD4⁺CD25⁻CD103⁻. One hundred nanograms (Fig. 7B, Expt. 1) or 5 ng (Fig. 7B, Expt. 2) of total RNA of each sample was reverse transcribed into cDNA by Superscript III first-strand synthesis kit (Invitrogen Life Technologies) and random hexamer primers, according to the manufacturer's instruction. The resultant cDNA was analyzed for the expression of Foxp3, IL-10, IFN- γ , and 18S rRNA using TaqMan Universal PCR Master Mix and Gene Expression Assay Mix (Applied Biosystems). Samples were amplified using the ABI Real-Time System (Applied Biosystems) or the Chromo4 Four-Color Real-Time PCR Detector (MJ Research; Bio-Rad). Sample cycle threshold (C_T) values were standardized to 18S rRNA values. The adjusted values were calculated based on the formula: 2^{-(C_T target - C_T 18S)} (26).

Statistical analysis

Statistical analysis for parasite numbers and cytokine values was performed using GraphPad Prism software and Student's *t* test at 95% confidence intervals, with differences considered significant at *, $p < 0.05$; **, $p < 0.01$; and ***, $p < 0.001$.

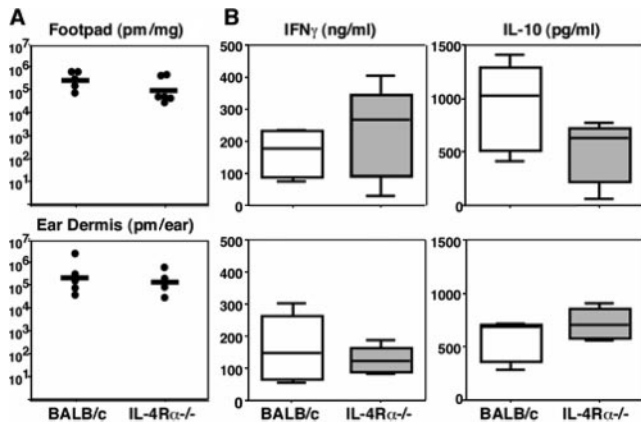


FIGURE 1. IL-4Rα^{-/-} mice remain susceptible to *L. major* LV39 in both footpad and ear dermal infections. BALB/c and IL-4Rα^{-/-} mice ($n = 5-6$ per group) were infected with 10^5 LV39 infectious metacyclic pm in the left hind footpad or 2×10^4 pm into both ears. Mice were sacrificed at day 48 postinfection, and parasite numbers were quantitated, as described in *Materials and Methods*. **A**, The numbers represent LV39 pm/mg infected footpad tissue (*top panel*) or total pm per ear (*bottom panel*). Each circle represents parasite numbers from an individual mouse tissue sample, and horizontal bars represent the geometric mean for each group. The figure is representative of four independent experiments. **B**, Draining LN cells (3×10^6 /ml) from footpad and dermis infections were stimulated with 25 μg/ml SLA for 72 h, and IFN-γ and IL-10 in culture supernatants were measured by ELISA. The results are represented as whisker boxes, showing the median, the 25th and 75th percentiles. The *upper* and *lower lines* represent the maximum and minimum values ($n = 5$). The experiment shown is representative of >10 experimental infections.

Results

IL-4Rα^{-/-} mice remain susceptible to L. major LV39 in footpad and ear dermis injection sites

We have established that genetically pure BALB/c IL-4Rα-deficient mice are highly susceptible to s.c. footpad injection of 10^5 infectious metacyclics of *L. major* substrain LV39. To investigate the mechanisms of *L. major* susceptibility within the site of infection, we used the ear dermal infection model initially described by Belkaid et al. (23). As shown in Fig. 1A, at day 48 postinfection, infected IL-4Rα^{-/-} mice were as susceptible as BALB/c mice with respect to parasite numbers in the footpad (pm/mg tissue), or infected ear dermis (total parasites/ear). Equivalent parasite numbers were also observed in the draining LN in both models of infection in IL-4Rα^{-/-} and BALB/c mice (data not shown). These results confirm that IL-4Rα^{-/-} mice remain susceptible to *L. major* LV39, regardless of the infection site, and both models can be

useful for evaluating the mechanisms of *L. major* susceptibility in the absence of IL-4/IL-13 signaling.

We have previously shown that IL-4Rα^{-/-} mice, while maintaining high numbers of parasites, had depressed levels of *L. major*-specific Th2 cytokines, including IL-10. In contrast to what would be predicted based on the Th1/Th2 paradigm, IL-4Rα^{-/-} mice did not default to a robust Th1 response with increased IFN-γ secretion (2). Fig. 1B shows that draining LN cells from IL-4Rα^{-/-} ear dermis infections (*bottom panel*) displayed similar trends and IFN-γ levels were not significantly elevated.

Although IL-10 secretion was somewhat increased in the IL-4Rα^{-/-} ear dermis draining LN after ex vivo SLA stimulation, the amounts of IL-10 were not statistically different from BALB/c levels. Therefore, the patterns of parasite growth and cytokine secretion are maintained in the ear dermis model of infection and can be used to dissect the cells and mechanisms promoting *L. major* susceptibility.

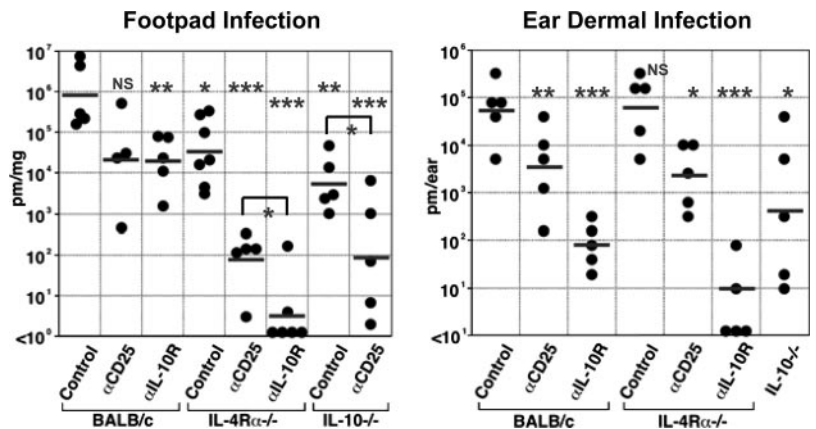
In vivo CD25 depletion partially controls L. major infection in IL-4Rα^{-/-} mice

We next examined the cellular source of IL-10 secretion in *L. major*-infected IL-4Rα^{-/-} mice. CD4⁺CD25⁺ T cells with a regulatory function have been shown to secrete IL-10 in both *L. major*-resistant and -susceptible mice (17, 20). We addressed the role of Treg cells in causing *L. major* susceptibility in IL-4Rα^{-/-} mice by in vivo depletion of Treg cells using anti-CD25 mAb and adoptive transfer of CD25-depleted T cell populations into IL-4Rα × RAG2 recipients.

BALB/c, IL-4Rα^{-/-}, and IL-10^{-/-} mice were given weekly injections of either anti-CD25 mAb (clone PC61.5.3) or anti-IL-10R mAb (clone 1B1.3a) during *L. major* infection, and parasite numbers were quantitated in the footpad and ear dermis (Fig. 2). If CD4⁺CD25⁺ T cells are the primary producers of IL-10, both anti-CD25 and anti-IL-10R treatments should lead to similar reductions in parasites in IL-4Rα^{-/-} mice.

After anti-IL-10R treatment, IL-4Rα^{-/-} mice were highly resistant to both footpad and dermal infections and contained ≈10,000- to 15,000-fold fewer *L. major* parasites than controls. Several IL-4Rα^{-/-} mice harbored no detectable parasites after 6-wk infection (Fig. 2). In parallel infections, BALB/c mice treated with anti-IL-10R showed some control of *L. major* growth with ≈40- and ≈700-fold decreases in footpad and ear dermis infection sites, respectively. Interestingly, BALB/c IL-10^{-/-} mice, which are resistant to *L. major* Friedlin strain (7), had only marginal reductions in *L. major* LV39 parasite numbers ($p < 0.05$ in dermal infection) and did not approach the highly resistant phenotype of anti-IL-10R-treated IL-4Rα^{-/-} mice ($p < 0.001$).

FIGURE 2. Anti-CD25 treatment partially inhibits *L. major* LV39 growth in footpad and dermal infections. BALB/c and IL-4Rα^{-/-} mice ($n = 4-6$ per group) were injected i.p. with 1 mg of anti-CD25 (PC61.5.3, rat IgG1), anti-IL-10R (1B1.3a, rat IgG1), or control IgG1 (GL113, rat IgG1) at day -3, day 0, and weekly during *L. major* LV39 infection. Mice were sacrificed, and parasite numbers from tissue lesions were quantitated at day 49 of footpad infection or day 43 of dermal infection. The numbers represent LV39 pm/mg infected footpad tissue or total pm per ear. The results shown represent one of two experiments. All Student's *t* test calculations were based on the BALB/c control group values. The efficiency of CD25 mAb treatment in LN and dermal populations was ≈90%. *, $p < 0.05$; **, $p < 0.01$; ***, $p < 0.001$.



Taken together, comparisons of anti-IL-10R-treated BALB/c and IL-4R $\alpha^{-/-}$ mice along with IL-10 $^{-/-}$ mice indicate that, regardless of the infection site, the full continuum of IL-10 and IL-4/IL-13 cytokines is involved in *L. major* LV39 susceptibility in BALB/c mice. These results also confirm that in the absence of IL-4/IL-13 signaling, susceptibility to *L. major* LV39 is mediated by IL-10, and resolution of the infection is induced by blocking IL-10R binding.

Although anti-IL-10R mAb was highly effective in reducing parasite numbers in IL-4R $\alpha^{-/-}$ mice, anti-CD25 mAb treatments did not achieve as impressive results, but did induce a significant 460-fold decrease in the footpad ($p < 0.001$) and 30-fold in the dermis ($p < 0.05$) (Fig. 2). In BALB/c mice, anti-CD25 produced only a 40-fold decrease of parasites in the footpad and 15-fold decrease in the dermis. The regimen of anti-CD25 mAb given in vivo was sufficient to deplete $\approx 90\%$ of the CD4 $^{+}$ CD25 $^{+}$ population, as measured by the inhibition of labeled PC61 mAb binding on LN and ear dermal cells taken 6 wk after *L. major* infection and 1 wk after the final anti-CD25 injection (data not shown). In addition, a recent publication shows that anti-CD25 mAb binding will effectively block Treg suppressor function and the capacity to bind IL-2 (27).

In contrast with our results, Aseffa et al. (21) demonstrated control of parasite growth in BALB/c mice treated with a single dose of 1 mg of anti-CD25 mAb 3 days before *L. major* infection. We compared both single- and multiple-dose anti-CD25 protocols in *L. major*-infected BALB/c and IL-4R $\alpha^{-/-}$ mice. Although parasite numbers in IL-4R $\alpha^{-/-}$ mice were decreased by multiple injections of anti-CD25 similar to those in Fig. 2, there was no change in the parasite burden of IL-4R $\alpha^{-/-}$ mice treated with a single dose of anti-CD25 mAb (data not shown).

Because CD25 functions as the IL-2R α -chain, anti-CD25 mAb may, in addition to altering Treg function, block the in vivo development of effector T cells that may either protect (Th1) or exacerbate (Th2) *L. major* disease progression. To address whether anti-CD25 mAb affects disease outcome independently of IL-10 secretion, we depleted CD25 $^{+}$ T cells in BALB/c IL-10 $^{-/-}$ mice. Fig. 2 shows that anti-CD25-treated IL-10 $^{-/-}$ mice contained 60-fold fewer parasites in the footpad lesions ($p < 0.05$), implying that anti-CD25 somewhat impedes the development of effector T cells, presumably IL-4- and IL-13-producing Th2 cells.

With regard to cytokine patterns, IFN- γ secretion was a more reliable indicator of successful parasite clearance in footpad infections than in the dermis model (Fig. 3). Footpad-infected IL-4R $\alpha^{-/-}$ mice had pronounced IFN- γ levels after both anti-CD25 and anti-IL-10R treatments (Fig. 3A). Anti-CD25 also induced an IFN- γ response in IL-10 $^{-/-}$ mice, suggesting that, along with IL-10-secreting Treg cells, a portion of the CD4 $^{+}$ CD25 $^{+}$ T population includes IL-4- or IL-13-secreting effector Th2 cells during *L. major* infection. We did not find statistical differences in the levels of IFN- γ in SLA-stimulated ear dermis LN cells (Fig. 3B).

As shown in Fig. 3, in both SLA-stimulated footpad and ear dermis LN populations, anti-IL-10R mAb-treated IL-4R $\alpha^{-/-}$ mice showed a significant decrease in IL-10 secretion compared with CD25 depletion ($p < 0.05$ for footpad LN and $p < 0.01$ for dermal LN). Dermal LN cultures from anti-IL-10R mAb-treated IL-4R $\alpha^{-/-}$ mice were also significantly reduced in IL-10 production compared with LN from anti-CD25 mAb mice ($p < 0.05$). Taken together, the data from the two infection models show that whereas blocking IL-10 activity is sufficient to resolve *L. major* infection in IL-4R $\alpha^{-/-}$ mice, depletion of CD4 $^{+}$ CD25 $^{+}$ T cells in vivo does not induce a similar resistant phenotype. This implies that CD4 $^{+}$ CD25 $^{+}$ T cells may be only a partial source of IL-10 in *L. major*

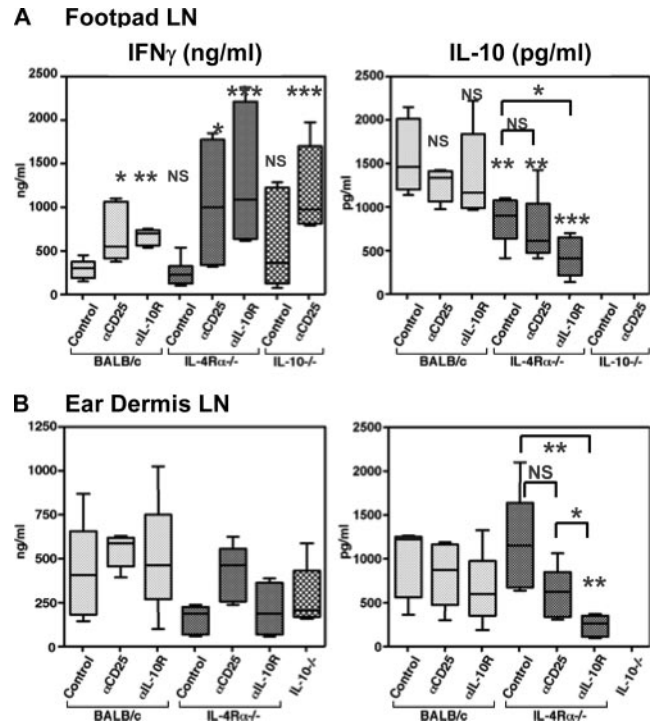


FIGURE 3. Up-regulation of IFN- γ after anti-CD25 treatment. Draining LN cells (3×10^6 /ml) from footpad (A) and dermis (B) infections shown in Fig. 2 were stimulated with 25 μ g/ml SLA for 72 h, and IFN- γ and IL-10 in culture supernatants were measured by ELISA. The results are represented as whisker boxes, showing the median, the 25th and 75th percentiles. The upper and lower lines represent the maximum and minimum values ($n \geq 5$). *, $p < 0.05$; **, $p < 0.01$; ***, $p < 0.001$.

LV39 susceptibility and indicate the existence of other sources of IL-10 that contribute to *L. major* parasite survival.

Adoptive transfer of CD4 $^{+}$ CD25 $^{-}$ T cells

We next asked whether transferring CD25-depleted T cells (CD4 $^{+}$ CD25 $^{-}$) into IL-4R \times RAG2 recipients would induce a resistant phenotype. In order to maintain susceptibility to *L. major* in IL-4R $\alpha \times$ RAG2-reconstituted mice, it was necessary to transfer a high dose of T cells. Varkila et al. (28) have shown that adoptive transfer of low numbers of T cells causes a healing phenotype in BALB/c SCID mice, whereas a high-dose (7.5×10^7) transfer of splenocytes leads to susceptibility. We therefore transferred 1×10^7 total naive CD4 $^{+}$ T cells from either IL-4R $\alpha^{-/-}$ or IL-4R $\alpha \times$ IL-10 double-knockout (KO) mice and compared these with mice reconstituted with 1×10^7 CD4 $^{+}$ CD25 $^{-}$ -purified cells from IL-4R $\alpha^{-/-}$ mice. The reconstituted recipients were infected with *L. major* LV39, and parasite burdens were compared with intact susceptible BALB/c, IL-4R $\alpha^{-/-}$, and IL-10 $^{-/-}$ mice and resistant IL-4R $\alpha \times$ IL-10 KO mice (Fig. 4).

As expected, the nonreconstituted IL-4R $\alpha \times$ RAG2 mice had uncontrolled infections and contained high numbers of parasites in the ear dermis 6 wk postinfection (Fig. 4). Reconstitution of the IL-4R $\alpha \times$ RAG2 mice with total CD4 cells from either IL-4R $\alpha^{-/-}$ or IL-4R $\alpha \times$ IL-10 KO mice restored the respective phenotypes observed in the intact susceptible and resistant mouse strains.

More importantly, mice reconstituted with 1×10^7 CD4 $^{+}$ CD25 $^{-}$ T cells were not resistant, and had comparable parasite numbers in the ear dermis to mice reconstituted with total CD4 $^{+}$ T cells. Although this may suggest CD4 $^{+}$ CD25 $^{-}$ T cells as a source of IL-10, it is also possible that CD25-negative Treg cells

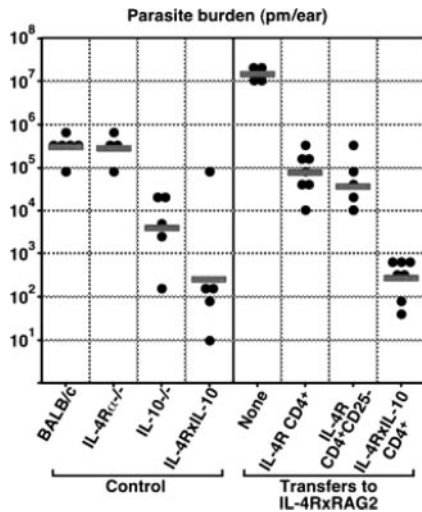


FIGURE 4. Transfer of CD25-depleted CD4⁺ T cells does not confer resistance to *L. major* LV39. IL-4Rα × RAG2 mice were injected i.v. with 10⁷ CD4⁺ or CD4⁺CD25⁻ T cells from naive IL-4Rα^{-/-} mice, or CD4⁺ T cells from naive IL-4R × IL-10 mice. Mice (*n* = 4–7 per group) were infected intradermally with 2 × 10⁴ *L. major* LV39 the day after reconstitution. Infected mice were sacrificed at day 42 postinfection, and the parasite numbers from ear dermis lesions were quantitated, as described in *Materials and Methods*. The results shown represent one of three experiments.

are induced to express CD25 upon transfer into a lymphopenic environment. Indeed, flow cytometric analysis revealed similar percentages of CD25⁺ cells in both total CD4⁺ and CD4⁺CD25⁻ reconstituted groups 6 wk after infection (data not shown). To address this, we reconstituted intact, naive IL-4Rα × IL-10 KO mice with 1 × 10⁵ FACS-purified CD4⁺CD25⁺CD103⁺ or CD4⁺CD25⁻CD103⁻ populations purified from the ear LN of *L. major*-infected IL-4Rα^{-/-} mice 1 day before *L. major* infection. However, even in the presence of *L. major*-primed CD4⁺ cells, IL-4Rα × IL-10 KO mice remained highly resistant to infection (data not shown).

Nevertheless, an important conclusion that can be drawn from the results in Fig. 4 is that IL-10 secretion during *L. major* infection is primarily from T cells, as indicated by comparable parasite numbers between intact, resistant IL-4Rα × IL-10 mice and the

Table I. Frequency of CD4⁺CD25⁺ T cells in BALB/c and IL-4Rα^{-/-} mice^a

Group	Lymph Node		Ear Dermis
	CD4 ⁺ CD25 ⁺ (%)	Number (×10 ⁶)	CD4 ⁺ CD25 ⁺ (%)
BALB/c	12.8 ± 0.4	2.1 ± 0.4	21.2 ± 4.0
IL-4Rα ^{-/-}	15.3 ± 0.7*	1.7 ± 0.5 ^{NS}	42.3 ± 1.3***

^a Values are shown as mean ± SE of each group (*n* = 5). NS, Not significant; *, *p* < 0.05; ***, *p* < 0.001.

recipient mice receiving IL-4Rα × IL-10 KO CD4⁺ T cells. Although we cannot discount IL-10 from non-T cell sources such as macrophages, dendritic cells, or B cells, clearly a T cell source of IL-10 is playing a predominant role in *L. major* susceptibility.

Increased CD4⁺CD25⁺ and CD4⁺Foxp3⁺ cells in infected IL-4Rα^{-/-} dermis

We next asked whether the frequencies of CD4⁺CD25⁺ were altered in the susceptible IL-4Rα^{-/-} mice, and examined both the site of infection and the respective draining LN. As anticipated, CD4⁺CD25⁺ T cells comprised the typical 10% of total CD4⁺ T cells in the LN of naive, uninfected BALB/c and IL-4Rα^{-/-} mice (data not shown). The frequency of CD4⁺CD25⁺ T cells in the IL-4Rα^{-/-} retromaxillary LN was slightly increased compared with BALB/c LN after *L. major* infection (15.3 vs 12.8%); however, the absolute number of CD4⁺CD25⁺ T cells was comparable (Fig. 5A and Table I).

In contrast to the draining LN populations, the percentage of CD4⁺CD25⁺ cells within the dermal infection site was increased 1.5- to 2-fold in IL-4Rα^{-/-} mice (Fig. 5A and Table I). Although we were not able to count absolute numbers of lymphocytes in these dermal cell preparations, the ≈4-fold increased CD4⁺ T cells (1.4 vs 5.2% of total FACS-collected cells) coupled with the 2-fold increased percentage of CD25⁺ T cells within the CD4⁺ T cell population ensures that *L. major*-infected IL-4Rα^{-/-} mice harbor greater numbers of CD4⁺CD25⁺ T cells at the site of infection.

To confirm whether CD4⁺CD25⁺ T cells in *L. major*-infected mice express the transcription factor Foxp3, the definitive marker for Treg cells (29), we performed intranuclear staining for Foxp3 on LN and processed ear dermal cells. Correlating with the

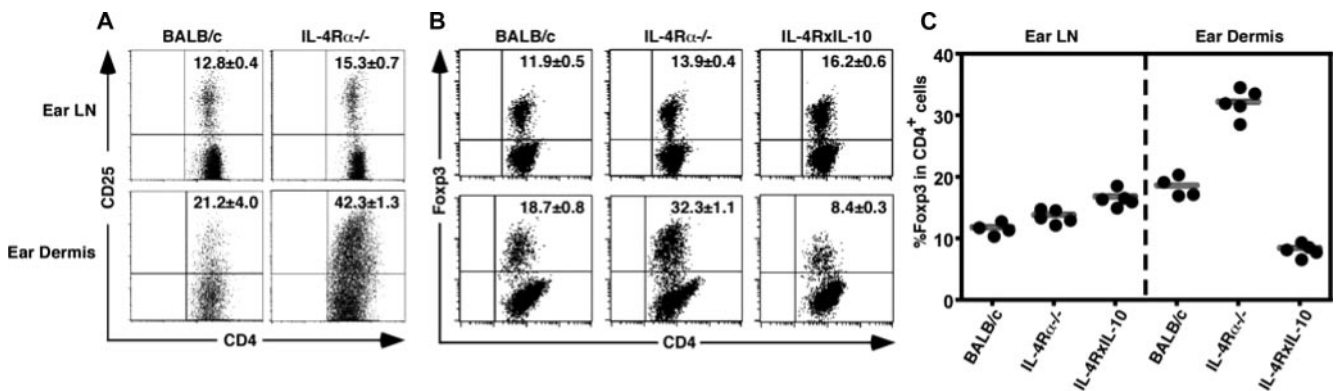


FIGURE 5. Increased percentages of CD4⁺CD25⁺ and CD4⁺Foxp3⁺ T cells in the dermis of susceptible IL-4Rα^{-/-} mice. LN and ear dermal cells were prepared from BALB/c, IL-4Rα^{-/-}, and IL-4Rα × IL-10 mice (*n* = 4–5 per group) 47 days after *L. major* LV39 infection and analyzed for CD25 (A) and Foxp3 (B) expression. Represented FACS profiles shown are gated on the CD4⁺ T cell population. Values indicate mean ± SE of CD25⁺ or Foxp3⁺ cell percentages of four to five mice per group. C, The percentages of Foxp3⁺ cells of individual mice are shown. Horizontal bars indicate the statistical mean of each group. The results shown represent one of four experiments measuring Foxp3 expression and >10 experiments measuring CD25 expression.

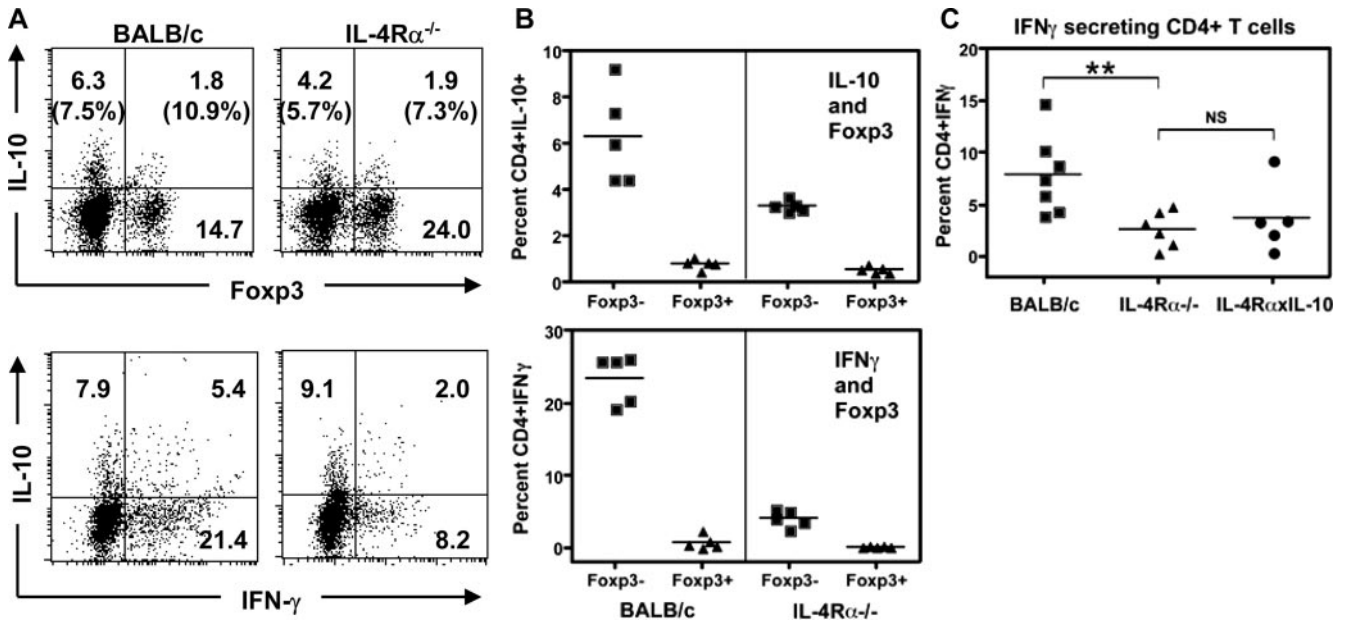


FIGURE 6. Fopx3-negative CD4⁺ cells are the predominate source of IL-10 in the dermis. **A**, Freshly isolated ear dermal cells from BALB/c and IL-4Rα^{-/-} mice infected for 6 wk with *L. major* LV39 were stimulated with 10 ng/ml PMA, 500 ng/ml ionomycin, and 3 mM monensin for 4 h. Stimulated cells were stained with combinations of mAbs detecting CD4, Fopx3, IL-10, and/or IFN-γ expression. Representative FACS profiles shown were gated on CD4⁺ cells obtained from 300,000 total accumulated events. The numbers within parenthesis are the percentages of IL-10-expressing cells within their respective CD4⁺Fopx3⁻ and CD4⁺Fopx3⁺ populations. **B**, In an independent infection, ear dermal cells from individual mice were stimulated, as described, and the percentages of Fopx3⁻ and Fopx3⁺ CD4⁺IL-10⁺ (top) and CD4⁺IFN-γ⁺ (bottom) populations were analyzed by FACS. **C**, In an additional experiment, the percentage of IFN-γ-secreting CD4⁺ T cells was enumerated in the infected dermis of BALB/c, IL-4Rα, and IL-4Rα × IL-10 KO mice. Each symbol represents the analysis of an individual infected mouse ear dermis homogenate. **, $p < 0.01$.

increase in CD4⁺CD25⁺ percentages, IL-4Rα^{-/-} mice consistently had 2-fold increased percentages of CD4⁺Fopx3⁺-expressing cells in the ear dermis (18.7 vs 32.2%; Fig. 5, *B* and *C*). As with CD25 expression, the increased Fopx3 expression was observed within the dermal infection site, but not in the draining LN. In addition to Fopx3, all the populations of CD4⁺CD25⁺ T cells that were analyzed, regardless of their location, expressed glucocorticoid-induced TNFR (30, 31) and CD103 (32), supporting a characteristic Treg phenotype (data not shown).

The apparent retention or accumulation of CD4⁺Fopx3⁺ cells in the infection site was more closely associated with the parasite load, rather than the absence of IL-4Rα. In highly resistant IL-4Rα × IL-10 KO mice, the percentage of CD4⁺Fopx3⁺ cells was remarkably low (8.4%) compared with IL-4Rα^{-/-} mice, or even with BALB/c mice (Fig. 5, *B* and *C*). The absence of all susceptibility pathways (IL-4/IL-13 and IL-10) in these mice permits efficient parasite killing by infected macrophages (Fig. 4).

IL-10 secretion from CD4⁺Fopx3⁻ non-Treg cells in infected IL-4Rα^{-/-} dermis

With the increase of CD4⁺Fopx3⁺ cells in the IL-4Rα^{-/-} ear dermis, we anticipated a concomitant increase in IL-10 secretion from CD4⁺Fopx3⁺ cells within the infection site as the cause of susceptibility in IL-4Rα^{-/-} mice. However, intracellular FACS analysis revealed that the percentage of IL-10-secreting CD4⁺ T cells within the IL-4Rα^{-/-}-infected ear dermis was not increased compared with BALB/c mice (Fig. 6A). Moreover, the majority of IL-10 was not produced by CD4⁺Fopx3⁺ cells, but rather by CD4⁺Fopx3⁻ cells, which comprised 6.3% of the CD4⁺ cells that produce IL-10 in the BALB/c dermis and 4.2% in the IL-4Rα^{-/-} dermis. Interestingly, the CD4⁺Fopx3⁻ and CD4⁺Fopx3⁺ populations contained comparable percentages of IL-10-expressing

cells (in parenthesis, Fig. 6A). In the retromaxillary draining LN of both BALB/c and IL-4Rα^{-/-} mice, IL-10 was also produced primarily by CD4⁺Fopx3⁻ cells (data not shown).

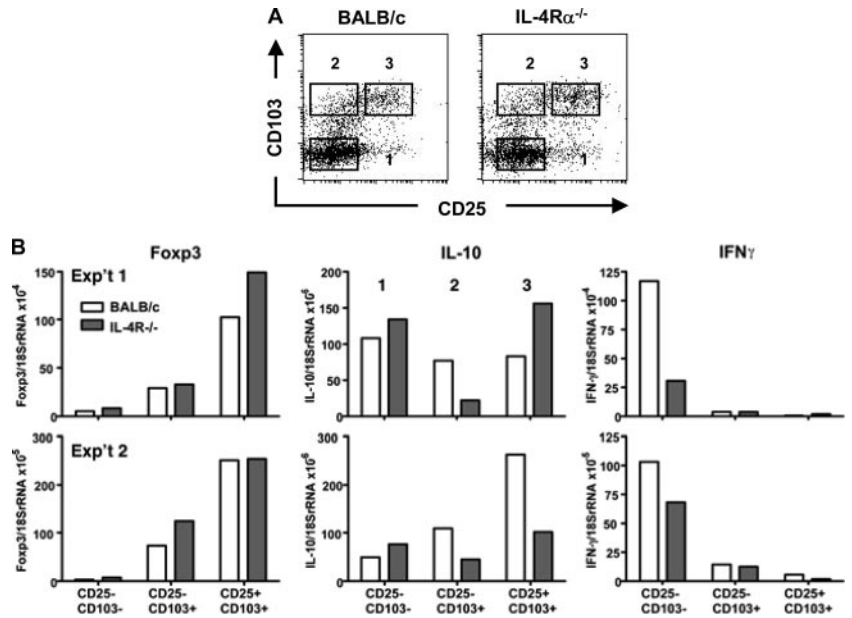
In the same analysis, CD4⁺ cells secreting IL-10 and IFN-γ were highly compartmentalized, with few cells producing both cytokines simultaneously (Fig. 6A, bottom panel). These data suggest that the IL-10-producing CD4⁺Fopx3⁻ cells are distinct from the IL-10/IFN-γ-secreting Th1 cells that have recently been described in *L. major*-infected C57BL/6 mice (22).

More striking was the depressed IFN-γ response in the IL-4Rα^{-/-} ear dermis, with only 8.2% of the CD4⁺ T cells expressing IFN-γ compared with 21.4% in the BALB/c dermis (Fig. 6A, bottom panel). This was also true, to a lesser extent, for the IFN-γ levels in supernatants of SLA-stimulated LN cells (Fig. 3), but not in PMA/ionomycin-stimulated LN cells (data not shown). In a separate experiment, CD4⁺ T cells in individual mouse ear dermis homogenates were analyzed for IL-10 and IFN-γ production (Fig. 6B). These results were also consistent with IL-10 secretion predominantly from CD4⁺Fopx3⁻ cells, and a suppressed IFN-γ response in the IL-4Rα^{-/-}-infected dermis.

A possible correlation of increased CD4⁺Fopx3⁺ Treg cells with suppressed IFN-γ responses is yet speculative. In highly resistant IL-4Rα × IL-10 KO mice, dermal IFN-γ production was not significantly increased compared with susceptible IL-4Rα single-deficient mice (Fig. 6C). However, this may be due to lack of *L. major* Ag stimulation and low numbers of inflammatory cells within the IL-4Rα × IL-10 KO dermis at 5- to 6-wk infection, when the lesions have resolved.

We next sorted CD4⁺ T cells isolated from the ear dermis based on cell surface CD4, CD25, and CD103 expression, and used real-time quantitative PCR (qPCR) to measure Fopx3, IL-10, and IFN-γ mRNA expression (Fig. 7). The expression of CD103, the α_Eβ₇ integrin, has been shown to accurately identify Treg subsets

FIGURE 7. Foxp3, IL-10, and IFN- γ mRNA expression in sorted CD4⁺ T cells from *L. major*-infected ear dermis (10 pooled ears). A, CD4⁺ T cells from the ear dermis of *L. major*-infected BALB/c and IL-4R α ^{-/-} mice were FACS sorted based on the expression of CD25 and CD103. All populations were sorted to >95% purity, and the CD25⁻CD103⁻ populations were >99% pure. B, Total RNA was extracted from FACS-sorted CD4⁺ cells based on expression of CD25 and CD103. The sorted populations from both *L. major*-infected BALB/c and IL-4R α ^{-/-} mice were reverse transcribed into cDNA, as described in *Materials and Methods*. cDNA was subjected to real-time qPCR using the TaqMan Probe system and Foxp3, IL-10, and IFN- γ primers and probes. Target values were normalized to 18S rRNA expression, and the relative values were calculated based on the $\Delta\Delta C_T$ method, as described in *Materials and Methods* (26). The qPCR results from two independent experimental infections are shown.



that may be CD4⁺CD25⁺ or CD4⁺CD25⁻, but express Foxp3 (32–34). The FACS-sort gated populations are shown in Fig. 7A. All populations were sorted to greater than 95% purity.

The qPCR results confirmed the cytokine and Foxp3 expression data obtained by intracellular staining and FACS. After *L. major* infection, both BALB/c and IL-4R α ^{-/-} mice had ~50-fold relative increases compared with uninfected controls in Foxp3 and IL-10 gene expression in the total ear dermis (data not shown). In mRNA isolated from highly purified CD4⁺ T cell populations from the ear dermis, the majority of Foxp3 expression was contained within the CD25⁺CD103⁺ populations, and was enriched ~3- to 67-fold in BALB/c and IL-4R α ^{-/-} mice compared with the CD25-negative populations (Fig. 7B, Expts. 1 and 2).

Interestingly, the qPCR profiles revealed similar levels of IL-10 mRNA expression between the CD25⁺CD103⁺ and CD25⁻CD103⁻ populations. Although these results may appear to be discordant with the FACS data shown in Fig. 6, the percentages of IL-10-secreting cells within the respective CD4⁺Foxp3⁻ and

CD4⁺Foxp3⁺ populations are comparable (Fig. 6A), and therefore the IL-10 qPCR results from sorted CD4⁺ populations are consistent with the FACS expression data.

With regard to IFN- γ levels, the mRNA expression was confined to the CD4⁺CD25⁻CD103⁻ population, indicating that IFN- γ expression is predominantly from the Foxp3⁻ and presumably, non-Treg cells, which we also observed by intracellular FACS analysis. The qPCR results also revealed suppressed IFN- γ mRNA levels in IL-4R α ^{-/-} CD4⁺CD25⁻CD103⁻ cells, which were 1.5- to 4-fold decreased compared with the BALB/c population (Fig. 7B).

IL-4 secretion was not detected in the ear dermis

We next assessed the nature of the IL-10-secreting CD4⁺Foxp3⁻ population in the ear dermis and whether they are conventional Th2 cells as measured by their capacity to also secrete IL-4. As shown in Fig. 8, there were low, but detectable numbers of CD4⁺ cells producing IL-4 in the BALB/c retromaxillary draining LN (*top*

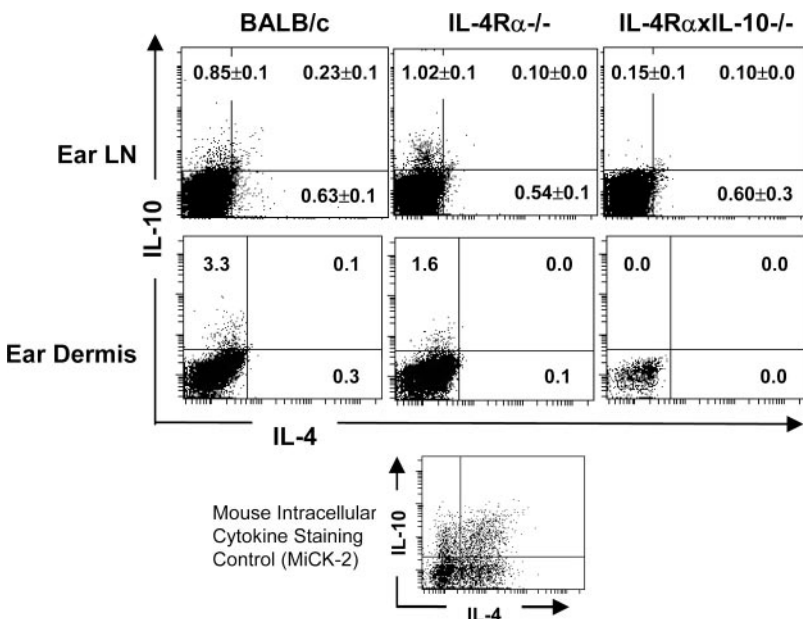


FIGURE 8. IL-10-producing CD4⁺ cells in *L. major*-infected dermis do not secrete IL-4. Groups of BALB/c, IL-4R α , and IL-4R α × IL-10 KO mice were infected for 5 wk with *L. major* LV39. Retromaxillary LN and ear dermis homogenates from infected mice were stimulated with 10 ng/ml PMA, 500 ng/ml ionomycin, and 3 mM monensin for 4 h. Retromaxillary LN from the infected groups of mice (4–5 mice per group) were individually analyzed for IL-10 and IL-4 production. Representative FACS profiles shown were gated on CD4⁺ cells obtained from 100,000 total accumulated events using the FACSCalibur and CellQuest analysis software. The percentage ± SD of IL-10 and IL-4 single producers and IL-10/IL-4 double-producing CD4⁺ T cells from individual analyzed LN is shown. Stimulated ear dermis homogenates from each group were pooled (*n* = 10 ears), and CD4⁺ T cells were analyzed for IL-10 and IL-4 production. Live gate was drawn on CD4-PerCP-stained cells vs side scatter, and at least 200,000 events were collected using the FACSaria. Data were analyzed using FACSDiva software. MiCK-2 cells (BD Biosciences) were used as cytokine-staining controls. The results shown represent one of three experiments.

panel) with very few IL-10/IL-4 double producers. In the ear dermis, IL-4 was not detectable in three separate infections (Fig. 8, bottom panel). The extremely low frequency of IL-4-producing CD4⁺ T cells in the ear dermis infection precludes a definitive characterization of the IL-10-secreting CD4⁺Foxp3⁻ cells as Th2 cells. Under the same stimulation and culture conditions, IL-10 and particularly robust IFN- γ production was observed (Fig. 6). qPCR measurements of the Th2-specific transcription factor GATA3 in CD25^{+/-}- and CD103^{+/-}-sorted populations were also inconclusive, because GATA3 was expressed in all sorted CD4⁺ populations from BALB/c and IL-4R α ^{-/-} dermis and LN (data not shown).

Discussion

Initially grouped within IL-4-driven Th2 cytokine responses, there is growing appreciation for an autonomous role of IL-10 in *L. major* infection. In mouse models of leishmaniasis, IL-10 secretion has been shown to be detrimental to infection with cutaneous strains such as *L. major*, *Leishmania mexicana*, and *Leishmania amazonensis* (6, 7, 35–37), and to the visceral strain *Leishmania donovani* (38–40). The dependence on IL-10 in determining disease outcome may also depend on the particular substrain of *L. major*, as has been documented with *L. major* LV39 (6) and *L. major* Seidman (35).

The mechanisms of induction and the cellular sources of IL-10 during infection are of considerable interest. In leishmaniasis, IL-10 may be secreted by conventional CD4⁺ T effector cells, CD4⁺CD25⁺ Treg cells (17), dendritic cells (41), and macrophages via FcR cross-linking (7, 42).

There has been recent attention given to CD4⁺CD25⁺ Treg cells in the pathogenesis of leishmaniasis and infectious diseases in general (43). There is not an overall consensus on what the function of natural Treg cells may be in *L. major* infection, and disparate experimental outcomes have frustrated attempts at creating a unifying model to explain *L. major* susceptibility. In *L. major*-resistant C57BL/6 mice, Belkaid et al. (17, 44) have shown that the IL-10-secreting CD4⁺CD25⁺ Treg function to maintain chronic infection to *L. major*/Friedlin and may be required to maintain immunological memory. Further studies showed that these cells maintain a Foxp3⁺ phenotype and recognize *L. major* Ags presented by infected dendritic cells (45). Anderson et al. (35) showed that CD4⁺CD25⁺ T cells promote susceptibility in C57BL/6 mice chronically infected with *L. major* NIH/Seidman substrain, but recently found that the CD4⁺CD25⁻Foxp3⁻ population was responsible for IL-10-mediated susceptibility (22). In contrast, Ji et al. (46) found CD4⁺CD25⁺ Treg cells to be beneficial for controlling *L. amazonensis* infections in C57BL/6 mice. In *L. major*-susceptible BALB/c mice, CD4⁺CD25⁺ Treg cells may either exacerbate (19) or protect (21) during infection.

In the absence of IL-4 and IL-13 responses, BALB/c IL-4R α ^{-/-} mice provide a useful model for elucidating the mechanisms of IL-10-mediated susceptibility in *L. major* infection. In these mice, IL-10 is the exclusive factor that promotes *L. major* LV39 parasite growth. Consistent with our previous findings in footpad infections (6), we show that in the ear dermis infection model, IL-4R α ^{-/-} mice depleted of IL-10 activity, either by anti-IL-10R mAb or by IL-10 gene deletion, are fully resistant to *L. major* LV39 (Fig. 2).

The results of T cell transfers shown in Fig. 4 also strongly suggest that CD4⁺ T cells are driving IL-10 responses in IL-4R α ^{-/-} mice, because naive CD4⁺ T cells isolated from either IL-4R α ^{-/-} (susceptible) or IL-4R α \times IL-10 (resistant) mouse strains transferred their respective disease outcomes to IL-4R α \times RAG2 mice. In previous experiments, we also found that IL-4R α ^{-/-} mice exhibited a healing phenotype after anti-CD4 mAb treatment at the time of infection (6).

Although T cell-derived IL-10 is critical for *L. major* parasite growth in IL-4R α ^{-/-} mice, the source of IL-10 is not confined to CD4⁺CD25⁺ Treg cells, as shown by comparing disease outcomes after anti-CD25 and anti-IL-10R mAb treatments in vivo, adoptive transfer of CD25-depleted CD4⁺ T cells into IL-4R α \times RAG2 KO mice, intracellular IL-10 and Foxp3 FACS analysis, and qPCR (Figs. 2, 4, 6, and 7). Indeed, a majority of IL-10 is secreted by CD4⁺Foxp3⁻ T cells in the dermis (Fig. 6). We have not, however, dismissed a role for Treg cells in promoting *L. major* susceptibility. Infected IL-4R α ^{-/-} mice consistently displayed a 1.5- to 2-fold increase in CD4⁺Foxp3⁺ Treg cells within the dermal site accompanied with suppressed IFN- γ responses compared with BALB/c mice (Figs. 5 and 6).

Based on the data, we propose a model of *L. major* susceptibility that is biased toward Th2 effector cells and IL-10-secreting non-Treg cells as the primary drivers of susceptibility, with Treg cells possibly contributing a localized, albeit IL-10-independent role. Within the lesion, IL-10 is primarily from CD4⁺Foxp3⁻ effector cells, with smaller amounts secreted by CD4⁺Foxp3⁺ Treg cells. Th2 effectors, IL-10-secreting cells, and Treg functions may be modulated by weekly injections of anti-CD25 or anti-IL-10R mAb in vivo. Based on our data, IFN- γ -secreting Th1 cells do not express CD25 or Foxp3, at least during the late stages of infection, and would not be directly affected by anti-CD25 mAb (Figs. 6 and 7). The increase in CD4⁺Foxp3⁺ Treg cells in the IL-4R α ^{-/-} dermis is abolished in resistant IL-4R α \times IL-10 KO mice, implying that upon IFN- γ -mediated killing of parasites, Treg cells are no longer retained at the site due to the lack of parasite Ag or appropriate stimulation by APCs.

The precise nature of the IL-10-secreting non-Treg effector cells in the BALB/c *L. major* dermal infection model remains unclear. Based on our data showing compartmentalized IFN- γ - and IL-10-secreting populations (Fig. 6), the IL-10-producing CD4⁺ T cells are distinct from the IL-10/IFN- γ -secreting Th1 cells recently described in C57BL/6 mice infected with *L. major* Seidman (22) or in another intracellular parasite infection with *Toxoplasma gondii* (47). Our attempts to characterize the IL-10 producers as Th2 cells were not fruitful because it was difficult to enumerate IL-4-producing cells within the dermal site by FACS analysis (Fig. 8), and the Th2-specific transcription factor GATA3 was found in all CD25^{+/-}- and CD103^{+/-}-sorted CD4⁺ populations from BALB/c and IL-4R α ^{-/-} dermis and LN (data not shown). Nonetheless, in the draining LN where IL-4 was detected, there were very few CD4⁺ cells that secreted both IL-10 and IL-4 (Fig. 8), suggesting that these are not Th2 cells.

Although the role of IL-10 in susceptibility of IL-4R α ^{-/-} mice is unequivocal, the increase in Treg cells in the IL-4R α ^{-/-} dermis compels us to speculate that Treg may suppress local IFN- γ responses through IL-10-independent mechanisms. This is supported by data from Foussat et al. (48), in which CD4⁺CD45RB^{low} cells, known to contain Treg cells, did not produce IL-10 themselves, but nevertheless suppressed inflammation indirectly by differentiating Tr1 cells to secrete IL-10. In recently described experimental *Schistosoma mansoni* infections, the Treg population was also found to direct the development of T effector responses to *S. mansoni* parasite eggs in an IL-10-independent fashion (49).

Alternatively, Treg cells may induce suppression by direct cell contact with effector Th1 cells, by altering APC function, or by TGF- β secretion (50). Although TGF- β has been noted in *L. major* disease progression (20), we and others have shown through gene deletion that the cytokines IL-4, IL-13, and IL-10 are predominate susceptibility factors in *L. major* LV39 infection (2, 3, 6, 51). The results of anti-IL-10 mAb-treated IL-4R α ^{-/-} mice and infections in IL-4R α \times IL-10 mice support this conclusion (Figs. 2 and 4).

The increased percentage of CD4⁺Foxp3⁺ T cells in the IL-4Rα^{-/-} dermis may be due to their retention in the infection site as a consequence of impaired IL-4/IL-13 signaling on T cells themselves or on non-T cells such as dendritic cells or macrophages, which are host cells for *L. major* infection. Because IL-4Rα × IL-10 mice are highly resistant to *L. major*, despite reduced numbers of dermal CD4⁺Foxp3⁺ T cells (Fig. 5) and low percentages of IFN-γ-secreting CD4⁺ T cells (Fig. 6C), we favor the hypothesis that the IL-4Rα deficiency promotes a retention or recruitment of Treg cells to the site, due to chronic Ag stimulation or stimulatory signals from infected APCs. Once the infection has cleared, as in the case of resistant IL-4Rα × IL-10 mice, the CD4⁺Foxp3⁺ T cells are no longer retained within the site. Interestingly, Yao et al. (52) have shown that dendritic cell production of IL-10 was inhibited by IL-4 signaling. In infection with *L. donovani*, a strain causing visceral leishmaniasis, splenic stromal cells were shown to promote the development of tolerogenic or regulatory dendritic cells that secreted IL-10 during this chronic infection (53). The same group has recently shown that the majority of T cell-derived IL-10 is also secreted by CD4⁺CD25⁻Foxp3⁻ cells in *L. donovani* infection (54).

Because BALB/c and IL-4Rα^{-/-} mice have similar parasite loads (Fig. 1), it is unlikely that exposure to *L. major* alone can be attributed to the increased Foxp3⁺ cells in the IL-4Rα^{-/-} dermis. We have, however, observed a pronounced increase in CD11b⁺ MHC class II^{high} cells in IL-4Rα^{-/-} dermal sites after *L. major* infection (data not shown). The increase in these cells was independent of adaptive immunity and was found in IL-4Rα × RAG2 KO ear dermis infected with *L. major* LV39. The CD11b⁺ MHC class II^{high} cells may allow for efficient retention of CD4⁺CD25⁺ T cells in the inflammatory site by providing efficient Ag presentation, or through the secretion of IL-10, chemokines, or expression of adhesion molecules such as E-cadherin, the ligand of CD103. In a mouse model of colitis, Uhlir et al. (55) have recently reported IL-10-secreting CD25⁺Foxp3⁺ cells in contact with MHC class II⁺ cells in the colon, suggesting an association of Treg cells with APCs not only in lymphoid tissues, but also within sites of tissue inflammation. In addition, Sather et al. (56) have shown that a high percentage of Treg cells with a CCR4⁺CD103^{high} phenotype is present in the skin and function to home to and prevent localized inflammatory disease in these tissues.

Taken together, BALB/c IL-4Rα^{-/-} mice, which are solely dependent on IL-10 for *L. major* susceptibility, reveal CD4⁺Foxp3⁻ cells as the major source of IL-10 in vivo. Nevertheless, the influx of CD4⁺Foxp3⁺ T cells within the IL-4Rα^{-/-} *L. major*-infected dermis implies an IL-10-independent role for Treg cells within the inflammatory site.

Acknowledgments

We thank Teresa Hawley (Flow-Cytometry Core Facility, George Washington University) for cell sorting and excellent technical advice, and Drs. Susana Mendez (Cornell University), David Sacks (National Institute of Allergy and Infectious Diseases, National Institutes of Health), David Leitenberg (George Washington University), and Achshah Keegan (University of Maryland) for their valuable advice and critical comments on the manuscript.

Disclosures

The authors have no financial conflict of interest.

References

- Sacks, D., and N. Noben-Trauth. 2002. The immunology of susceptibility and resistance to *Leishmania major* in mice. *Nat. Rev. Immunol.* 2: 845–858.
- Noben-Trauth, N., W. E. Paul, and D. L. Sacks. 1999. IL-4- and IL-4 receptor-deficient BALB/c mice reveal differences in susceptibility to *Leishmania major* parasite substrains. *J. Immunol.* 162: 6132–6140.
- Matthews, D. J., C. L. Emson, G. J. McKenzie, H. E. Jolin, J. M. Blackwell, and A. N. McKenzie. 2000. IL-13 is a susceptibility factor for *Leishmania major* infection. *J. Immunol.* 164: 1458–1462.
- Noben-Trauth, N., P. Kropf, and I. Muller. 1996. Susceptibility to *Leishmania major* infection in interleukin-4-deficient mice. *Science* 271: 987–990.
- Kropf, P., R. Etges, L. Schopf, C. Chung, J. Sypek, and I. Muller. 1997. Characterization of T cell-mediated responses in nonhealing and healing *Leishmania major* infections in the absence of endogenous IL-4. *J. Immunol.* 159: 3434–3443.
- Noben-Trauth, N., R. Lira, H. Nagase, W. E. Paul, and D. L. Sacks. 2003. The relative contribution of IL-4 receptor signaling and IL-10 to susceptibility to *Leishmania major*. *J. Immunol.* 170: 5152–5158.
- Kane, M. M., and D. M. Mosser. 2001. The role of IL-10 in promoting disease progression in leishmaniasis. *J. Immunol.* 166: 1141–1147.
- Belkaid, Y., K. F. Hoffmann, S. Mendez, S. Kamhawi, M. C. Udey, T. A. Wynn, and D. L. Sacks. 2001. The role of interleukin (IL)-10 in the persistence of *Leishmania major* in the skin after healing and the therapeutic potential of anti-IL-10 receptor antibody for sterile cure. *J. Exp. Med.* 194: 1497–1506.
- Shevach, E. M. 2002. CD4⁺CD25⁺ suppressor T cells: more questions than answers. *Nat. Rev. Immunol.* 2: 389–400.
- Sakaguchi, S. 2004. Naturally arising CD4⁺ regulatory T cells for immunologic self-tolerance and negative control of immune responses. *Annu. Rev. Immunol.* 22: 531–562.
- Fontenot, J. D., M. A. Gavin, and A. Y. Rudensky. 2003. Foxp3 programs the development and function of CD4⁺CD25⁺ regulatory T cells. *Nat. Immunol.* 4: 330–336.
- Zhang, X., L. Izikson, L. Liu, and H. L. Weiner. 2001. Activation of CD25⁺CD4⁺ regulatory T cells by oral antigen administration. *J. Immunol.* 167: 4245–4253.
- Apostolou, I., A. Sarukhan, L. Klein, and H. von Boehmer. 2002. Origin of regulatory T cells with known specificity for antigen. *Nat. Immunol.* 3: 756–763.
- Bluestone, J. A., and A. K. Abbas. 2003. Natural versus adaptive regulatory T cells. *Nat. Rev. Immunol.* 3: 253–257.
- Chen, W., W. Jin, N. Hardegen, K. J. Lei, L. Li, N. Marinos, G. McGrady, and S. M. Wahl. 2003. Conversion of peripheral CD4⁺CD25⁻ naive T cells to CD4⁺CD25⁺ regulatory T cells by TGF-β induction of transcription factor Foxp3. *J. Exp. Med.* 198: 1875–1886.
- Zheng, S. G., J. H. Wang, J. D. Gray, H. Soucier, and D. A. Horwitz. 2004. Natural and induced CD4⁺CD25⁺ cells educate CD4⁺CD25⁻ cells to develop suppressive activity: the role of IL-2, TGF-β, and IL-10. *J. Immunol.* 172: 5213–5221.
- Belkaid, Y., C. A. Piccirillo, S. Mendez, E. M. Shevach, and D. L. Sacks. 2002. CD4⁺CD25⁺ regulatory T cells control *Leishmania major* persistence and immunity. *Nature* 420: 502–507.
- Powrie, F., R. Correa-Oliveira, S. Mauze, and R. L. Coffman. 1994. Regulatory interactions between CD45RB^{high} and CD45RB^{low} CD4⁺ T cells are important for the balance between protective and pathogenic cell-mediated immunity. *J. Exp. Med.* 179: 589–600.
- Xu, D., H. Liu, M. Komai-Koma, C. Campbell, C. McSharry, J. Alexander, and F. Y. Liew. 2003. CD4⁺CD25⁺ regulatory T cells suppress differentiation and functions of Th1 and Th2 cells, *Leishmania major* infection, and colitis in mice. *J. Immunol.* 170: 394–399.
- Liu, H., B. Hu, D. Xu, and F. Y. Liew. 2003. CD4⁺CD25⁺ regulatory T cells cure murine colitis: the role of IL-10, TGF-β, and CTLA4. *J. Immunol.* 171: 5012–5017.
- Aseffa, A., A. Gumy, P. Launois, H. R. MacDonald, J. A. Louis, and F. Tacchini-Cottier. 2002. The early IL-4 response to *Leishmania major* and the resulting Th2 cell maturation steering progressive disease in BALB/c mice are subject to the control of regulatory CD4⁺CD25⁺ T cells. *J. Immunol.* 169: 3232–3241.
- Anderson, C. F., M. Oukka, V. J. Kuchroo, and D. Sacks. 2007. CD4⁺CD25⁺Foxp3⁻ Th1 cells are the source of IL-10-mediated immune suppression in chronic cutaneous leishmaniasis. *J. Exp. Med.* 204: 285–297.
- Belkaid, Y., S. Kamhawi, G. Modi, J. Valenzuela, N. Noben-Trauth, E. Rowton, J. Ribeiro, and D. L. Sacks. 1998. Development of a natural model of cutaneous leishmaniasis: powerful effects of vector saliva and saliva preexposure on the long-term outcome of *Leishmania major* infection in the mouse ear dermis. *J. Exp. Med.* 188: 1941–1953.
- Noben-Trauth, N., L. D. Shultz, F. Brombacher, J. F. Urban, Jr., H. Gu, and W. E. Paul. 1997. An interleukin 4 (IL-4)-independent pathway for CD4⁺ T cell IL-4 production is revealed in IL-4 receptor-deficient mice. *Proc. Natl. Acad. Sci. USA* 94: 10838–10843.
- Spath, G. F., and S. M. Beverley. 2001. A lipophosphoglycan-independent method for isolation of infective *Leishmania* metacyclic promastigotes by density gradient centrifugation. *Exp. Parasitol.* 99: 97–103.
- Livak, K. J., and T. D. Schmittgen. 2001. Analysis of relative gene expression data using real-time quantitative PCR and the 2(-ΔΔC(T)) method. *Methods* 25: 402–408.
- Kohm, A. P., J. S. McMahon, J. R. Podojil, W. S. Begolka, M. Degutes, D. J. Kasprovicz, S. F. Ziegler, and S. D. Miller. 2006. Cutting edge: anti-CD25 monoclonal antibody injection results in the functional inactivation, not depletion, of CD4⁺CD25⁺ T regulatory cells. *J. Immunol.* 176: 3301–3305.
- Varkila, K., R. Chatelain, L. M. Leal, and R. L. Coffman. 1993. Reconstitution of C.B-17 scid mice with BALB/c T cells initiates a T helper type-1 response and renders them capable of healing *Leishmania major* infection. *Eur. J. Immunol.* 23: 262–268.

29. Hori, S., T. Nomura, and S. Sakaguchi. 2003. Control of regulatory T cell development by the transcription factor Foxp3. *Science* 299: 1057–1061.
30. Shimizu, J., S. Yamazaki, T. Takahashi, Y. Ishida, and S. Sakaguchi. 2002. Stimulation of CD25⁺CD4⁺ regulatory T cells through GITR breaks immunological self-tolerance. *Nat. Immunol.* 3: 135–142.
31. McHugh, R. S., M. J. Whitters, C. A. Piccirillo, D. A. Young, E. M. Shevach, M. Collins, and M. C. Byrne. 2002. CD4⁺CD25⁺ immunoregulatory T cells: gene expression analysis reveals a functional role for the glucocorticoid-induced TNF receptor. *Immunity* 16: 311–323.
32. Huehn, J., K. Siegmund, J. C. Lehmann, C. Siewert, U. Haubold, M. Feuerer, G. F. Debes, J. Lauber, O. Frey, G. K. Przybylski, et al. 2004. Developmental stage, phenotype, and migration distinguish naive- and effector/memory-like CD4⁺ regulatory T cells. *J. Exp. Med.* 199: 303–313.
33. Lehmann, J., J. Huehn, M. de la Rosa, F. Maszyra, U. Kretschmer, V. Krenn, M. Brunner, A. Scheffold, and A. Hamann. 2002. Expression of the integrin $\alpha_E\beta_7$ identifies unique subsets of CD25⁺ as well as CD25⁻ regulatory T cells. *Proc. Natl. Acad. Sci. USA* 99: 13031–13036.
34. Suffia, I., S. K. Reckling, G. Salay, and Y. Belkaid. 2005. A role for CD103 in the retention of CD4⁺CD25⁺ Treg and control of *Leishmania major* infection. *J. Immunol.* 174: 5444–5455.
35. Anderson, C. F., S. Mendez, and D. L. Sacks. 2005. Nonhealing infection despite Th1 polarization produced by a strain of *Leishmania major* in C57BL/6 mice. *J. Immunol.* 174: 2934–2941.
36. Padigel, U. M., J. Alexander, and J. P. Farrell. 2003. The role of interleukin-10 in susceptibility of BALB/c mice to infection with *Leishmania mexicana* and *Leishmania amazonensis*. *J. Immunol.* 171: 3705–3710.
37. Buxbaum, L. U., and P. Scott. 2005. Interleukin 10- and Fc γ receptor-deficient mice resolve *Leishmania mexicana* lesions. *Infect. Immun.* 73: 2101–2108.
38. Murphy, M. L., U. Wille, E. N. Villegas, C. A. Hunter, and J. P. Farrell. 2001. IL-10 mediates susceptibility to *Leishmania donovani* infection. *Eur. J. Immunol.* 31: 2848–2856.
39. Murray, H. W., C. M. Lu, S. Mauze, S. Freeman, A. L. Moreira, G. Kaplan, and R. L. Coffman. 2002. Interleukin-10 (IL-10) in experimental visceral leishmaniasis and IL-10 receptor blockade as immunotherapy. *Infect. Immun.* 70: 6284–6293.
40. Murray, H. W., K. C. Flanders, D. D. Donaldson, J. P. Sypek, P. J. Gotwals, J. Liu, and X. Ma. 2005. Antagonizing deactivating cytokines to enhance host defense and chemotherapy in experimental visceral leishmaniasis. *Infect. Immun.* 73: 3903–3911.
41. Qi, H., V. Popov, and L. Soong. 2001. *Leishmania amazonensis*-dendritic cell interactions in vitro and the priming of parasite-specific CD4⁺ T cells in vivo. *J. Immunol.* 167: 4534–4542.
42. Miles, S. A., S. M. Conrad, R. G. Alves, S. M. Jeronimo, and D. M. Mosser. 2005. A role for IgG immune complexes during infection with the intracellular pathogen *Leishmania*. *J. Exp. Med.* 201: 747–754.
43. Belkaid, Y., and B. T. Rouse. 2005. Natural regulatory T cells in infectious disease. *Nat. Immunol.* 6: 353–360.
44. Mendez, S., S. K. Reckling, C. A. Piccirillo, D. Sacks, and Y. Belkaid. 2004. Role for CD4⁺CD25⁺ regulatory T cells in reactivation of persistent leishmaniasis and control of concomitant immunity. *J. Exp. Med.* 200: 201–210.
45. Suffia, I. J., S. K. Reckling, C. A. Piccirillo, R. S. Goldszmid, and Y. Belkaid. 2006. Infected site-restricted Foxp3⁺ natural regulatory T cells are specific for microbial antigens. *J. Exp. Med.* 203: 777–788.
46. Ji, J., J. Masterson, J. Sun, and L. Soong. 2005. CD4⁺CD25⁺ regulatory T cells restrain pathogenic responses during *Leishmania amazonensis* infection. *J. Immunol.* 174: 7147–7153.
47. Jankovic, D., M. C. Kullberg, C. G. Feng, R. S. Goldszmid, C. M. Collazo, M. Wilson, T. A. Wynn, M. Kamanaka, R. A. Flavell, and A. Sher. 2007. Conventional T-bet⁺Foxp3⁻ Th1 cells are the major source of host-protective regulatory IL-10 during intracellular protozoan infection. *J. Exp. Med.* 204: 273–283.
48. Foussat, A., F. Cottrez, V. Brun, N. Fournier, J. P. Breittmayer, and H. Groux. 2003. A comparative study between T regulatory type 1 and CD4⁺CD25⁺ T cells in the control of inflammation. *J. Immunol.* 171: 5018–5026.
49. Baumgart, M., F. Tompkins, J. Leng, and M. Hesse. 2006. Naturally occurring CD4⁺Foxp3⁺ regulatory T cells are an essential, IL-10-independent part of the immunoregulatory network in *Schistosoma mansoni* egg-induced inflammation. *J. Immunol.* 176: 5374–5387.
50. Von Boehmer, H. 2005. Mechanisms of suppression by suppressor T cells. *Nat. Immunol.* 6: 338–344.
51. Mohrs, M., C. Holscher, and F. Brombacher. 2000. Interleukin-4 receptor α -deficient BALB/c mice show an unimpaired T helper 2 polarization in response to *Leishmania major* infection. *Infect. Immun.* 68: 1773–1780.
52. Yao, Y., W. Li, M. H. Kaplan, and C. H. Chang. 2005. Interleukin (IL)-4 inhibits IL-10 to promote IL-12 production by dendritic cells. *J. Exp. Med.* 201: 1899–1903.
53. Svensson, M., A. Maroof, M. Ato, and P. M. Kaye. 2004. Stromal cells direct local differentiation of regulatory dendritic cells. *Immunity* 21: 805–816.
54. Stager, S., A. Maroof, S. Zubairi, S. L. Sanos, M. Kopf, and P. M. Kaye. 2006. Distinct roles for IL-6 and IL-12p40 in mediating protection against *Leishmania donovani* and the expansion of IL-10⁺ CD4⁺ T cells. *Eur. J. Immunol.* 36: 1764–1771.
55. Uhlig, H. H., J. Coombes, C. Mottet, A. Izcue, C. Thompson, A. Fanger, A. Tannapel, J. D. Fontenot, F. Ramsdell, and F. Powrie. 2006. Characterization of Foxp3⁺CD4⁺CD25⁺ and IL-10-secreting CD4⁺CD25⁺ T cells during cure of colitis. *J. Immunol.* 177: 5852–5860.
56. Sather, B. D., P. Treuting, N. Perdue, M. Miazgowica, J. D. Fontenot, A. Y. Rudensky, and D. J. Campbell. 2007. Altering the distribution of Foxp3⁺ regulatory T cells results in tissue-specific inflammatory disease. *J. Exp. Med.* 204: 1335–1347.